Philosophical Magazine
Publication details, including instructions for authors and subscription information:
http://www.tandfonline.com/loi/tphm20

Implementation of a new Fe-He three-body interatomic potential for molecular dynamics simulations

R.E. Stoller [a], S.I. Golubov [a b], P.J. Kamenski [c], T. Seletskaia [a] & Yu.N. Osetsky [a]

[a] Materials Science and Technology Division, Oak Ridge National Laboratory, Oak Ridge, TN 37831-6138, USA

[b] Department of Materials Science and Engineering, University of Tennessee, Knoxville, TN, USA

[c] Department of Materials Science and Engineering, University of Wisconsin, Madison, WI, USA

Published online: 30 Mar 2010.

To cite this article: R.E. Stoller, S.I. Golubov, P.J. Kamenski, T. Seletskaia & Yu.N. Osetsky (2010) Implementation of a new Fe-He three-body interatomic potential for molecular dynamics simulations, Philosophical Magazine, 90:7-8, 923-934, DOI: 10.1080/14786430903298768

To link to this article: http://dx.doi.org/10.1080/14786430903298768

Philosophical Magazine
Vol. 90, Nos. 7–8, 7–14 March 2010, 923–934

Taylor & Francis
Taylor & Francis Group

Implementation of a new Fe–He three-body interatomic potential for molecular dynamics simulations

R.E. Stoller[a]*, S.I. Golubov[ab], P.J. Kamenski[c†], T. Seletskaia[a] and Yu.N. Osetsky[a]

[a]*Materials Science and Technology Division, Oak Ridge National Laboratory, Oak Ridge, TN 37831-6138, USA;* [b]*Department of Materials Science and Engineering, University of Tennessee, Knoxville, TN, USA;* [c]*Department of Materials Science and Engineering, University of Wisconsin, Madison, WI, USA*

(*Received 9 July 2009; final version received 28 August 2009*)

A recently developed interatomic potential for He–Fe interactions includes a three-body term to stabilize the interstitial He defect in the tetrahedral position in the Fe bcc matrix and provides simultaneous agreement with the forces and energies of different atomic configurations as computed by first principles. This term makes a significant contribution to the static and dynamic properties of He in Fe. The implementation of this potential for atomistic simulations using molecular dynamics (MD) presented certain challenges which are discussed here to facilitate its further use in materials research, particularly to investigate the behavior of iron-based alloys that may be employed in fusion energy systems. Detailed results of an MD study comparing the new potential and alternate He–Fe pair potentials with different iron matrix potentials have been presented elsewhere to illustrate the impact of the He–Fe potential on He diffusion, helium clustering and the dynamics of He-vacancy clusters.

Keywords: bubbles; helium effects; irradiated materials; microstructure; multiscale modeling; iron; helium

1. Introduction

Helium produced by nuclear transmutation has a substantial impact on radiation-induced microstructural evolution [1–4] and is, therefore, a concern for DT fusion reactor environments. Since no current irradiation facility can produce prototypical levels of helium and atomic displacements, computational modeling and simulation plays a primary role in understanding the impact of helium. Although computational tools have advanced appreciably in recent years, most relevant atomistic work on the effects of helium in iron have employed a relatively old pair potential to describe the He–Fe interactions [5]. The underlying assumption of the adequacy of a pair

*Corresponding author. Email: rkn@ornl.gov
†Current address: University of Oxford, Oxford, UK.

ISSN 1478–6435 print/ISSN 1478–6443 online

DOI: 10.1080/14786430903298768
http://www.informaworld.com

potential to describe these interactions was challenged by recent *ab initio* calculations [6,7], leading to the development of a three-body Fe–He interatomic potential [8,9]. This potential was fitted to an extensive database of properties calculated by first principles, including the forces on atoms and the energies of different configurations of He in the bcc Fe matrix and He-vacancy clusters. To simultaneously fit both the forces and energies and obtain the tetrahedral position in the bcc lattice as the stable site for the He interstitial defect required a three-body angular dependent term in the Fe–He interaction potential [9]. This term contributes significantly to all the properties of He atoms in the Fe matrix such as the formation energy and defect configurations at zero temperature as well as diffusion and interactions between He atoms and other defects at non-zero temperatures. The potential is currently being used in an extensive investigation of He transport and He-bubble properties which includes a direct comparison with the available pair potentials [5,10]. Significant differences have been found between the predictions obtained with the various potentials [11]. A preliminary description of the three-body interactions was presented in [9]. However, implementation of the three-body interactions in a fast and efficient molecular dynamics (MD) scheme is not obvious. The purpose of this report is to facilitate usage of the new He–Fe interatomic potential by providing complete details on the three-body He–Fe interactions and their contribution to He behavior in the Fe matrix and a description of the implementation of the three-body interactions in an MD simulation code.

2. Description of Fe–He three-body potential

2.1. *Total potential energy*

The total potential energy of a Fe crystal doped with He is given by

$$U_{\text{total}} = \sum_{i=1}^{I_{\text{Fe}}} U_{\text{Fe}}(\rho_i) + \sum_{i=1}^{I_{\text{Fe}}-1} \sum_{j=i+1}^{I_{\text{Fe}}} U_{\text{FeFe}}(r_{ij}) + \sum_{i=1}^{I_{\text{He}}-1} \sum_{j=i+1}^{I_{\text{He}}} U_{\text{HeHe}}(r_{ij}) + \sum_{i=1}^{I_{\text{He}}} \sum_{j=1}^{I_{\text{Fe}}} U_{\text{HeFe}}(r_{ij}) + \sum_{i=1}^{I_{\text{He}}} \sum_{j=1}^{I_{\text{Fe}}-1} \sum_{k=j+1}^{I_{\text{Fe}}} U_{\text{HeFeFe}}(r_{ij}, r_{ik}, \theta_{jik}). \quad (1)$$

The first and second summation terms in Equation (1) correspond to a pure iron, embedded atom potential. Three different iron matrix potentials have been studied, including the Finnis and Sinclair potential [12], the 1997 Ackland et al. potential [13], and the 2004 Ackland et al. potential [14]. The third term on the right-hand side of Equation (1) describes helium–helium interactions through the pair potential developed by Aziz et al. [15]. The last two terms on the right-hand side of Equation (1) correspond to two-body helium–iron interactions and three-body iron–helium–iron interactions. This report shall clarify the implementation and impact of these last two terms in Equation (1).

Note that the variable and function names in Equation (1) reflect conventional usage to simplify the following discussion. The summation index description on the right-hand side of the equation is different from that written in [9] to correct

errors which would otherwise lead to double-counting of certain pair and triplet contributions.

2.2. *Two-body He–Fe interaction*

The helium–iron two-body potential energy is given by

$$U_{\mathrm{HeFe}} = \begin{cases} \exp(b_1 + b_2 r_{ij} + b_3 r_{ij}^2 + b_4 r_{ij}^3 + b_5 r_{ij}^4), & r_{ij} < 1.6, \\ a_1 + a_2 r_{ij} + a_3 r_{ij}^2 + a_4 r_{ij}^3 + a_5 r_{ij}^4 + a_6 r_{ij}^5, & 1.6 \le r_{ij} < 2.2, \\ p_1 \exp\left(-p_4\left(\dfrac{r_{ij}}{p_3} - 1\right)\right), & 2.2 \le r_{ij} < 4.1, \\ p_1 \exp\left(-p_4\left(\dfrac{r_{ij}}{p_3} - 1\right)\right)(1-\lambda)^3(1 + 3\lambda + 6\lambda^2), & 4.1 \le r_{ij} < 4.4, \end{cases} \tag{2}$$

where r_{ij} is the distance between He, (i), and Fe atom, (j), given by

$$r_{ij} = \sqrt{(x_j - x_i)^2 + (y_j - y_i)^2 + (z_j - z_i)^2}. \tag{3}$$

The variable λ in Equation (2) is related to r_{ij} as follows:

$$\lambda = \frac{r_{ij} - r_b}{r_c - r_b}, \tag{4}$$

where the parameters r_b and r_c are cutoff parameters given in Table 1. The parameters a, b, and p in Equation (2) are also presented in Table 1. The distances and energies in Equation (2) are given in Angstroms and eV, respectively. To be clear, in this summary, lowercase x variables correspond to the x positions of atoms. Note that the parameter p_2 in Equation (2) in [9] was omitted here since it was fit to be zero.

The forces on He and Fe atoms arising from the two-body potential (2) can be calculated using

$$\vec{F} = -\nabla U. \tag{5}$$

Taking into account the Newton's third law,

$$\vec{F}_i = -\vec{F}_j. \tag{6}$$

Based on Equation (6), it is sufficient to calculate the force acting on only one of the Fe (or the He) atoms. Taking into account Equation (5), the x-component

Table 1. Parameters for pair potential given by Equation (2).

$b_1 = -2.142600207811$	$a_1 = -285.7450302953$	$p_1 = 0.167753$
$b_2 = 32.965470333178$	$a_2 = 794.5913355517$	$p_2 = 0.00$
$b_3 = -52.893449935488$	$a_3 = -856.9376372455$	$p_3 = 2.432258$
$b_4 = 30.970079966695$	$a_4 = 452.5323035795$	$p_4 = 3.727249$
$b_5 = -6.398785336260$	$a_5 = -117.6519447529$	$r_b = 4.1$
	$a_6 = 12.0878858024$	$r_c = 4.4$

of the force on the j-th atom is given by

$$(F_j)_x = \begin{cases} -U_{\mathrm{HeFe}}(b_2 + 2b_3 r_{ij} + 3b_4 r_{ij}^2 + 4b_5 r_{ij}^3)\left(\dfrac{x_j - x_i}{r_{ij}}\right), & r_{ij} < 1.6, \\ -(a_2 + 2a_3 r_{ij} + 3a_4 r_{ij}^2 + 4a_5 r_{ij}^3 + 5a_6 r_{ij}^4)\left(\dfrac{x_j - x_i}{r_{ij}}\right), & 1.6 \le r_{ij} < 2.2, \\ p_1 \exp\left(-p_4\left(\dfrac{r_{ij}}{p_3} - 1\right)\right)\dfrac{(x_j - x_i)}{r_{ij}}\left[\dfrac{p_4}{p_3}\right], & 2.2 \le r_{ij} < 4.1, \\ p_1 \exp\left(-p_4\left(\dfrac{r_{ij}}{p_3} - 1\right)\right)\dfrac{(x_j - x_i)}{r_{ij}}\left[\dfrac{30}{r_c - r_b}\lambda^2(1-\lambda)^2 + \dfrac{p_4}{p_3}\left[(1-\lambda)^3(1 + 3\lambda + 6\lambda^2)\right]\right]. \\ \quad 4.1 \le r_{ij} < 4.4. \end{cases} \tag{7}$$

Forces in the y- and z-directions can be calculated by replacing the x_j and x_i terms with the corresponding y_j and y_i or z_j and z_i values, respectively. The force on the i atom, F_i, is given by Equation (6).

2.3. *Three-body He–Fe–Fe interaction*

The potential energy function for the helium–iron–iron three-body interaction is given by

$$U_{\mathrm{HeFeFe}}(r_{ij}, r_{ik}, \theta_{jik}) = f(r_{ij}) f(r_{ik}) \cos^2(\theta_{jik} - \chi), \tag{8}$$

where r_{ij} and r_{ik} are the distances between the helium atom located at a position (i) and two Fe atoms located at positions (j) and (k), respectively, and θ_{jik} is the angle between the corresponding vectors $\vec{r}_{ij}$ and $\vec{r}_{ik}$. The function $f(r)$ is given by

$$f(r) = \begin{cases} \alpha, & r \le r_{b3}, \\ \alpha(1 - \Lambda)^3(1 + 3\Lambda + 6\Lambda^2), & r_{b3} < r \le r_{c3}, \end{cases} \tag{9}$$

$$\Lambda = \frac{r - r_{b3}}{r_{c3} - r_{b3}}, \tag{10}$$

where the parameters α, r_{b3} and r_{c3} are given in Table 2 together with the parameter χ. Note that the angle θ_{jik} varies from zero to π.

Taking into account that the distances r_{ij} and r_{ik} are determined by the coordinates of atoms as follows:

$$\begin{aligned} r_{ij} &= \sqrt{(x_j - x_i)^2 + (y_j - y_i)^2 + (z_j - z_i)^2}, \\ r_{ik} &= \sqrt{(x_k - x_i)^2 + (y_k - y_i)^2 + (z_k - z_i)^2}, \end{aligned} \tag{11}$$

Table 2. Parameters for three-body potential given by Equations (8) and (9).

α	0.7
r_{b3}	1.75
r_{c3}	2.2
χ	0.44

the angle θ_{jik} is given by

$$\theta_{jik} = \arccos\left(\frac{(x_j - x_i)(x_k - x_i) + (y_j - y_i)(y_k - y_i) + (z_j - z_i)(z_k - z_i)}{r_{ij} r_{ik}}\right). \quad (12)$$

It can be also shown that Newton's third law in the case takes the following form:

$$\vec{F}_i = -(\vec{F}_j + \vec{F}_k). \quad (13)$$

Thus, it is enough to calculate forces on two atoms only, e.g. on two Fe atoms. Using Equation (5), the x-component of the force acting on the j-Fe atom can be presented as follows:

$$\begin{aligned}(F_j)_x = &-\left(\frac{df(r_{ij})}{\mathrm{d}x_j}\right) f(r_{ik}) \cos^2(\theta_{jik} - \chi) \\ &- f(r_{ij}) f(r_{ik}) \frac{\sin(2(\theta_{jik} - \chi))}{\sin(\theta_{jik})} \frac{\mathrm{d}\cos(\theta_{jik})}{\mathrm{d}x_j},\end{aligned} \quad (14)$$

where

$$\begin{aligned}\frac{\mathrm{d}f(r_{ij})}{\mathrm{d}x_j} &= \begin{cases} 0, & r_{ij} \le r_{b3}, \\ -30\alpha\Lambda^2(1-\Lambda)^2 \dfrac{(x_j - x_i)}{r_{ij}(r_{c3} - r_{b3})}, & r_{b3} < r_{ij} \le r_{c3}, \\ 0, & r_{ij} \ge r_{c3}, \end{cases} \\ \frac{\mathrm{d}\cos(\theta_{jik})}{\mathrm{d}x_j} &= \frac{(x_k - x_i)}{r_{ij} r_{ik}} - \cos(\theta_{jik}) \frac{(x_j - x_i)}{r_{ij}^2}.\end{aligned} \quad (15)$$

The y and z components of the force can be obtained from Equations (14) and (15) by replacing x-coordinates with y- and z-coordinates, respectively. The force acting on the k-Fe atom can be obtained from the same equations by replacing j-coordinates with k-coordinates and vice versa. Finally, the force acting on the He atom is given by Equation (13). Note that the $\sin(\theta_{jik})$ factor in the denominator of Equation (14) will go to zero if $\theta_{jik} = \pi$. As a practical matter of the implementation, we have set a cutoff value of θ_{jik} that is close to π, 3.141583, to prevent numerical instability and have verified that this has no significant impact on the results.

Thus, the set of Equations (1)–(15) can be used in conjunction with any of the interatomic potentials for the iron matrix published in [12–14] and the He–He interaction described in [15] to obtain a full and comprehensive description of the potential energy and forces acting on He and Fe atoms in an Fe crystal doped with He.

2.4. *Energy and force acting on the He atom in a given triplet configuration*

The complex nature of the forces and the energy landscape for a given Fe–He–Fe triplet are illustrated in Figures 1–3, which are presented to provide a visualization of the three-body potential. The results are from calculations for a single Fe–He–Fe triplet. The most significant observation that can be drawn from these figures is the strong angular dependence of the three-body term. The angular dependence and value of χ were chosen to guarantee the tetrahedral site provided the lowest

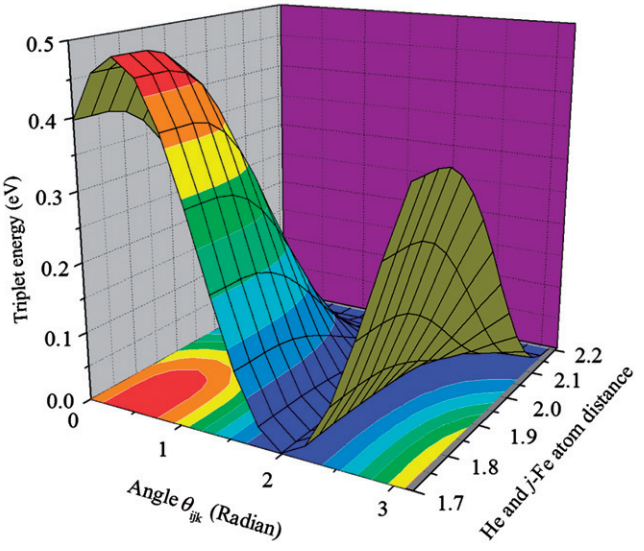

Figure 1. Energy of Fe–He–Fe triplet as a function of θ and r_{ik}, where r_{ij} is equal to 1.8 Å.

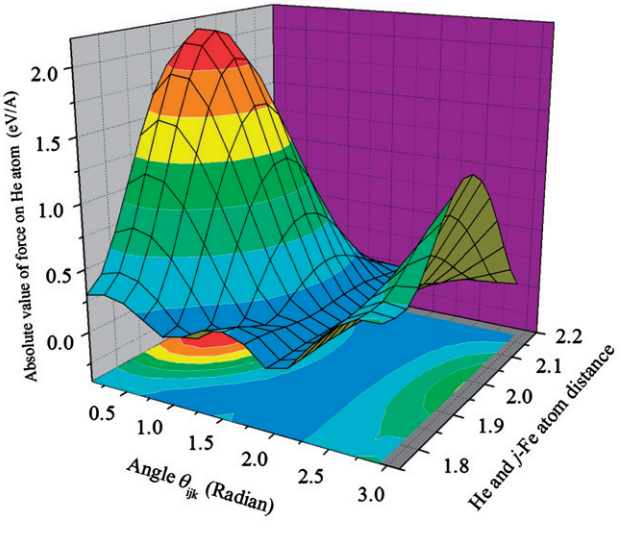

Figure 2. Absolute value of the force acting on the He atom as a function of θ and r_{ik}, where r_{ij} is equal to 1.8 Å.

interstitial formation energy. This leads to a relatively weak dependence on the distance between helium and either iron atom in the triplet when the angle is near that associated with the tetrahedral location, $\theta_{jik} \sim 1.92$ rad. For example, the energy minimum of the Fe–He–Fe triplet at this angle shown in Figure 1 only weakly depends on the He–Fe separation but varies strongly with the angle. The absolute force on the helium atom is similarly minimized as shown in Figure 2. The decision

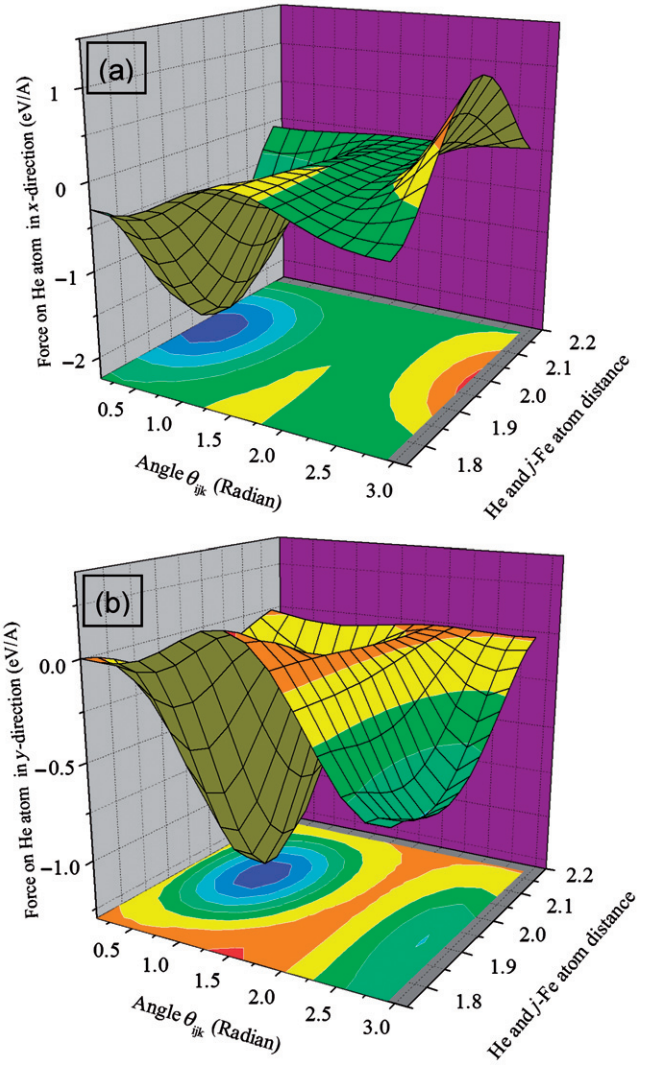

Figure 3. Force acting on the He atom in the (a) x-direction and (b) y-direction in the x–y-plane as a function of θ and r_{ik}, where r_{ij} is equal to 1.8 Å.

to use the triplet angle to stabilize the tetrahedral interstitial is in contrast to the recent pair potential by Juslin and Nordlund [10] in which a steep radial (He–Fe spacing) dependence was used to accomplish this. A comparison of the two approaches has yielded significant differences in the static properties of He-vacancy clusters, migration of interstitial He in the Fe matrix, and the kinetics of He- and He-vacancy cluster evolution as described in [11].

Additional information on the forces on a helium atom near the tetrahedral position is given in Figure 3, which shows the forces in two principle directions for a helium atom located in a {100} plane. In both cases, the force is near zero and relatively insensitive to He–Fe distance near the specified angle.

3. Influence of three-body term on He atom migration

The influence of the three-body term on the He migration path is shown in Figures 4–8, for which the calculations were done for one He atom in an unrelaxed Fe lattice. Figure 4 shows the energy change for a He atom passing from one

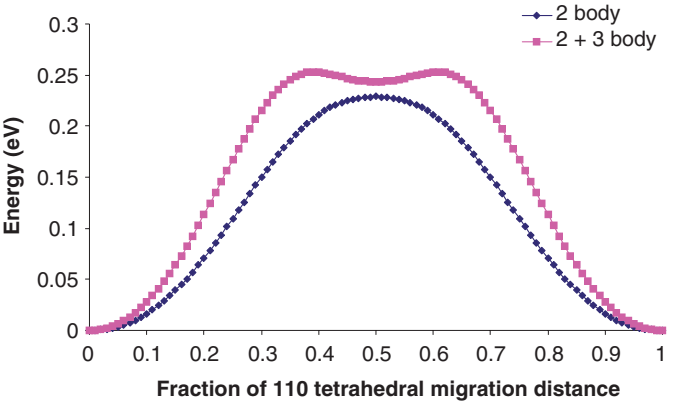

Figure 4. (Color online). Migration energy barrier for a He atom passing from one tetrahedral site to another along a ⟨110⟩ direction. Note that both energy curves have been shifted such that the He atom in the tetrahedral sites has an energy equal to zero. This data is obtained for an unrelaxed lattice.

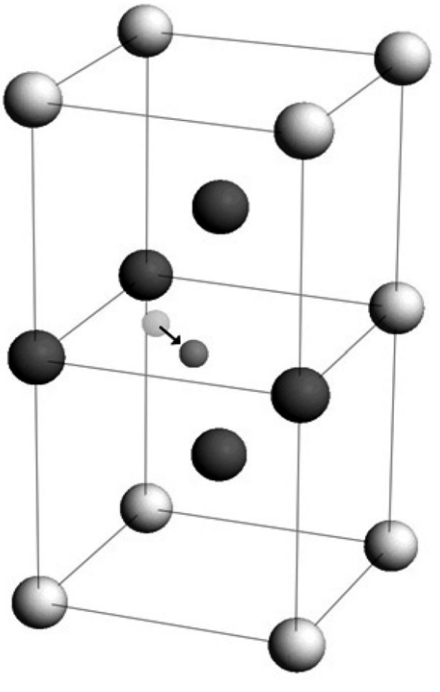

Figure 5. ⟨110⟩ He migration in bcc Fe. The five nearest neighbors during this migration are darkened. Provided by Dr. Y. Matsukawa, ORNL (now University of Illinois).

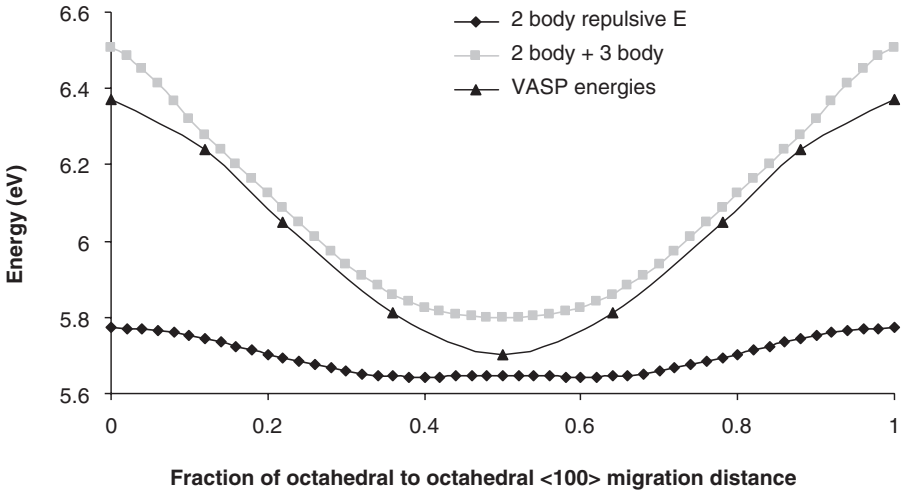

Figure 6. Energy of a He atom moving along a ⟨100⟩ direction from one octahedral site to another. Note that the He atom goes through a tetrahedral site mid-way. This data is for an unrelaxed lattice.

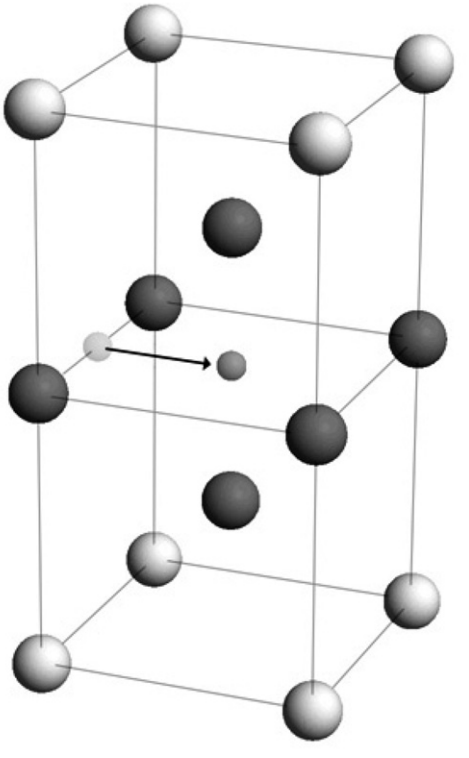

Figure 7. ⟨100⟩ Octahedral interstitial He migration in bcc Fe. The six nearest neighbors for the final octahedral configuration are darkened. Provided by Dr. Y. Matsukawa, ORNL (now University of Illinois).

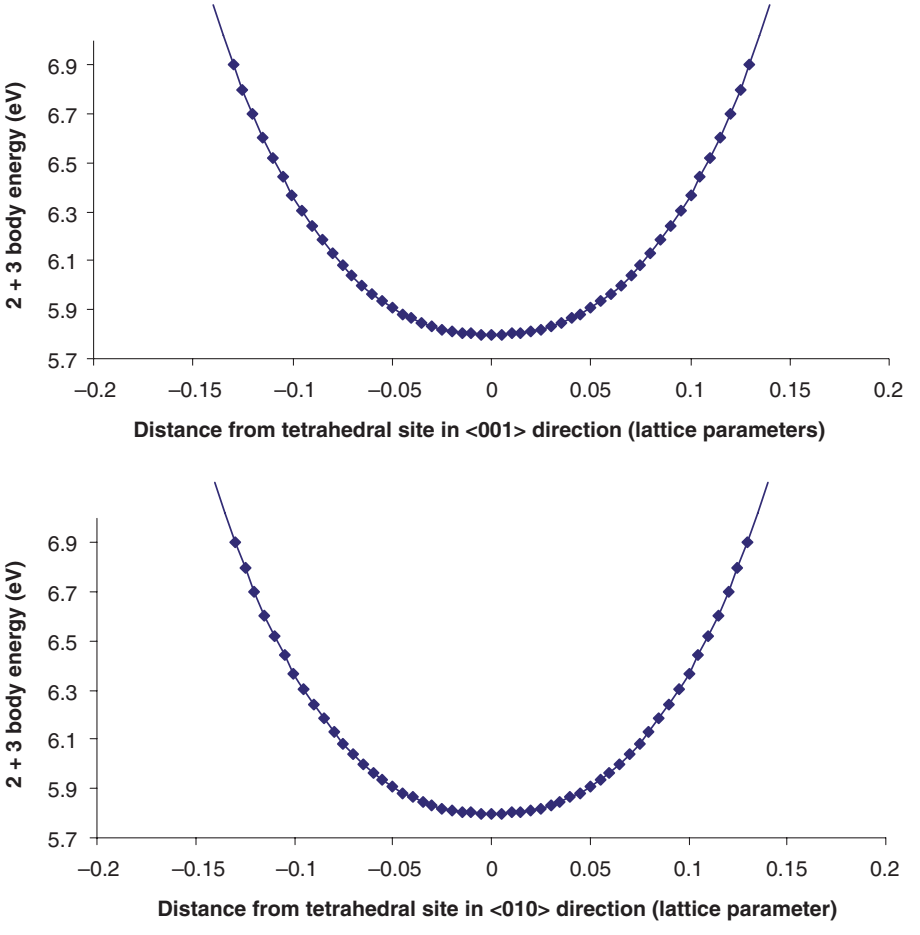

Figure 8. Energy of a He atom moving along the other two principle directions relative to Figures 6 and 7, showing the tetrahedral site as a local energy minimum in each principle direction.

tetrahedral site to another along a ⟨110⟩ direction (illustrated in Figure 5), which is the energetically favored migration path [7,9]. It is clear that the addition of the three-body term changes both the magnitude and the shape of the energy barrier. The local energy minimum produced in the intermediate region in the case of three-body potential relates to the types of Fe–He–Fe triplets that arise in this intermediate configuration. The five nearest neighbors in this region are shown in Figure 5. The energy barrier for the unrelaxed lattice shown in Figure 4 (~0.25 eV) is higher than the *ab initio* result of 0.06 eV. Calculations for a relaxed lattice reported in [9] yielded values of 0.03, 0.04, and 0.03 eV when the three-body He-Fe potential was combined with the Finnis–Sinclair [12], 1997 Ackland, et al. [13] and 2004 Ackland, et al. [14] iron potentials, respectively. Although these are large relative differences, all the values are quite low on an absolute energy scale, leading to essentially athermal migration.

The Fe–He–Fe triplets formed in the intermediate region either (a) form an angle close to the preferential angle, and/or (b) have at least one long distance vector. Both (a) and (b) lead to smaller energy contributions for the given triplet. So, instead of a smooth energy barrier for migration given by the purely repulsive two-body potential shown in the figure, the three-body contribution produces a meta-stable triangular site found half way through the migration, as shown Figure 5.

The migration path described energetically in Figure 6 can be seen in Figure 7. The two-body repulsive energy shown in Figure 7 produces an octahedral to tetrahedral site energy difference of 124 meV. When the three-body term is added, the energy difference is 711 meV, which is much closer to the VASP energy difference of 670 meV. Also, the two-body repulsive potential makes the tetrahedral site a local energy maximum (by a small amount), whereas with the three-body term added, the tetrahedral site is a local energy minimum. This migration path from one octahedral site directly to another passes through a tetrahedral site, which is mid-way through the motion. The energy minimum along this path is clearly the tetrahedral site. The energy landscape for He migration along the ⟨010⟩ and ⟨001⟩ orthogonal (relative to Figures 6 and 7) principle directions is shown in Figure 8, illustrating that the tetrahedral site is a local energy minimum in each principle direction.

4. Summary

The procedure, equations and coefficients necessary to implement a new Fe–He three-body potential [9] have been described. Moreover, the description provides a general way to understand three-body interactions in atomistic simulations. The energy landscape provided by this new potential is substantially more complex than that of a simple pair potential, and provides results in good agreement with *ab initio* calculations. The importance of three-body interactions for He migration and stabilization of the tetrahedral configuration is demonstrated, and the use of the new potential is recommended. As an example of its impact, [11] describes a detailed investigation of the behavior of He and He-vacancy clusters in which results obtained with this three-body potential are compared with those obtained using pair potentials.

Acknowledgements

Research sponsored by the Division of Materials Sciences (RES, TS, and YNO) and Engineering and the Office of Fusion Energy Sciences (SIG, PJK), US Department of Energy, under contract DE-AC05-00OR22725 with UT-Battelle, LLC.

References

[1] R.E. Stoller, J. Nucl. Mater 174 (1990) p.289.
[2] R.E. Stoller and G.R. Odette, J. Nucl. Mater. 154 (1988) p.286.
[3] R.E. Stoller, P.J. Maziasz, A.F. Rowcliffe and M.P. Tanaka, J. Nucl. Mater 155/157 (1988) p.1328.

[4] R.E. Stoller and G.R. Odette, *A comparison of the relative importance of helium and vacancy accumulation in void nucleation*, in *Radiation-Induced Changes in Microstructure, ASTM STP 955*, F.A. Garner, N.H. Packan and A.S. Kumar, eds., American Society of Testing and Materials, Philadelphia, 1987, p.358.
[5] W.D. Wilson and R.A. Johnson, *Rare gases in metals*, in *Interatomic Potentials and Simulation of Lattice Defects*, P.C. Gehlen, J.R. Beeler and R.J. Jaffee, eds., Battelle Institute Materials Science Colloquia, Columbus, Ohio, 1972, p.375.
[6] T. Seletskaia, Yu.N. Osetsky, R.E. Stoller and G.M. Stocks, Phys. Rev. Lett. 94 (2005) p.046403.
[7] Chu-Chun Fu and F. Willaime, Phys. Rev. B. 72 (2005) p.064117.
[8] T. Seletskaia, Yu.N. Osetsky, R.E. Stoller and G.M. Stocks, J. Nucl. Mater 351 (2006) p.109.
[9] T. Seletskaia, Yu.N. Osetsky, R.E. Stoller and G.M. Stocks, J. Nucl. Mater 367/370 (2007) p.355.
[10] N. Juslin and K. Nordlund, J. Nucl. Mater 382 (2008) p.143.
[11] D.M. Stewart, S.I. Golubov, Yu.N. Ostesky, R.E. Stoller, T. Seletskaia and P.J. Kamenski, Phil. Mag. 90 (2010) p.941.
[12] M.W. Finnis and J.E. Sinclair, Philos. Mag. A 50 (1984) p.45.
[13] G.J. Ackland, D.J. Bacon, A.F. Calder and T. Harry, Phil. Mag. A 75 (1997) p.713.
[14] G.J. Ackland, M.I. Mendelev, D.J. Srolovitz, S. Han and A.V. Barashev, J. Phys. Condens. Matter 16 (2004) p.S2629.
[15] R.A. Aziz, A.R. Janzen and M.R. Moldovan, Phys. Rev. Let. 74 (1995) p.1586.